



Synthesis and petrophysical characterization of an artificial mudstone analogous

Raquel Fedrizzi¹, Marco Ceia¹, Roseane Misságia¹, Victor Santos¹, Irineu Lima Neto², ¹UENF/LENEP ²Fundenor

Copyright 2017, SBGf - Sociedade Brasileira de Geofísica

This paper was prepared for presentation during the 15th International Congress of the Brazilian Geophysical Society held in Rio de Janeiro, Brazil, 31 July to 3 August, 2017.

Contents of this paper were reviewed by the Technical Committee of the 15th International Congress of the Brazilian Geophysical Society and do not necessarily represent any position of the SBGf, its officers or members. Electronic reproduction or storage of any part of this paper for commercial purposes without the written consent of the Brazilian Geophysical Society is prohibited.

Abstract

Carbonate rocks are important for rock properties research because they are linked to significant oil and gas reserves around the world. The goal of synthesizing carbonate rocks in laboratory is to simulate the natural carbonate rock matrix regarding the main factors of lithification such as grain size and shape, concentration of cementing material and compaction pressure, and allowing the production of rock specimens that can be used for tests in extreme conditions in replacement of the high cost natural cores. The reproduction of rocks in laboratory also allows to access samples with predetermined characteristics enabling a better understanding of the relationship between their physical properties. In this work, samples of synthetic carbonate rocks were made by mixing a fixed amount of calcite and sand, and varying the amount of cement material (Portland cement and water). The behavior of the main petrophysical characteristics of these samples was investigated, such as porosity, permeability and P- and S-wave velocities versus the amount of cementing material. The results were compared with natural carbonate samples and showed a high similarity to the petrophysical behavior of natural mudstones rocks.

Introduction

Carbonate rocks have a great importance to the worldwide petroleum industry, accounting approximately 50% of the world's total hydrocarbon production (Xu and Payne, 2009). These rocks cover a range of depositional facies, with considerable textural variability and complex porous media, showing a diversity of pore types, a wide range of pore sizes, and heterogeneity which hamper the correlative analysis of its physical properties, such as porosity, permeability, elastic velocities and mineralogical composition.

Core samples of natural rocks are required for several types of tests in petroleum engineering research as core flooding performance evaluation for Enhanced Oil Recovery (EOR) techniques and formation damage investigations (Torsater et al., 2013; Sacramento et al., 2015) that may change their original characteristics, and geomechanical essays that can be destructive. As coring

operations have a high cost, the synthesis of artificial carbonate rocks in lab environment allows the access to rock samples with analog predetermined characteristics to natural rocks, but with a relatively lower cost. Additionally, it is difficult to obtain representative carbonate samples and quantify their pore structures due to the complex pore system and high heterogeneity. Thereafter, carbonate rocks have not been intensely investigated from the rock physics properties perspective.

On the other hand, manufacturing physical models with previously known porous system allows researchers to simulate natural limestone matrix regarding the main factors of lithification as grain size and shape, the concentration of cementing materials and compression pressure. Those issues can provide the basis for quantitatively studying the pore structure effects on acoustic and petrophysical properties at ultrasonic scale.

There are many techniques available in the literature to synthesize sandstones that explored the influence of sand grain selection, type of cement and vertical compaction pressure (Den Brok et al., 1997; David et al., 1998), but few studies dealing with synthetic limestone (Piane et al. 2015; Wang et al., 2015). Niraula (2004) used crushed limestone, Portland cement and water for producing artificial core plugs to be used in rock mechanics simulations. El Husseiny and Vanorio (2015) used cold-pressing of different mixtures of coarse and very fine calcite grains to produce synthetic micritic carbonate analogs for CO₂ injection tests.

In this work, carbonate rocks were made using a combination of sand, calcite, Portland cement and water. We investigated the behavior of porosity, permeability and P- and S- waves of those rocks versus the amount of cementing material. For some of the samples, we also investigated the pore space structured through pore size distribution from Mercury Injection Porosimetry (MIP) and digital image analysis of petrographical images. The results were compared with the reported for natural mudstones and showed analogous petrophysical characteristics.

Method

Our artificial samples aimed to reproduce carbonates with primary interparticle porosity. The materials used to produce the synthetic rocks were: calcite, sand, Portland cement and water. The calcite and sand content in the artificial samples were based on previous experiments with natural carbonate rocks (Lima Neto et al., 2014) that had reported a composition of approximately 95% of calcite/dolomite and 5% of quartz. The used sand was previously sieved to separate grains with average sizes of 0.3 and 0.15 millimeters.

To prepare the samples, the dry mass of the aggregate (calcite and sand) was pre-weighed. Afterward, the cement and water percentages were based on the aggregate weight (Table 1). The artificial samples were manufactured through three different methods detailed hereafter. To understand the petrophysical and acoustic behavior of the manufactured samples, the amount of cement and/or water were varied.

In all the procedures, a mixer was used to blend the mineral aggregate and cementing fluid to ensure a homogeneous cover of the surface grains by the cementing fluid. The mixture was uniformly placed into a mold and was subjected to a mechanical compression for 24 hours using a hydraulic press (Figure 1). After removing the samples from the molds, they were placed in an oven and maintained for 24 hours heated to 100°C. After that, the temperature was increased 25°C per hour until it reaches 300°C. Finally, the samples are cooled down to ambient temperature and could be used for testing.

First method

The first method consisted of testing the influence of cementing fluid content in the rock properties. Thus, five samples were manufactured with different cement (20-60%) and water (10-40%) contents. In this method, we used only the sand with average grain size of 0.3 mm.

A cylindrical mold was used and the mechanical compression of 25.8 MPa was applied.

Second method

This method was conceived to test the effect of a mixture of sands with different average grain sizes on the physical properties of the rocks. Three samples were produced. Half of the amount of the used sand content was related to 0.3 mm grain size (3 grams) and the other half filled with 0.15 mm grain size (3 grams). The cylindrical mold was also used and the mechanical compression was the same of the first method. The cement content varied from 40-60% while the water content ranges from 20-40%.

Third method

This method was proposed to test the repeatability of the artificial samples. Hence, a carbonate block was produced measuring 10 cm height and 15 cm length. The compaction pressure used was approximately 5.23 MPa. It was not possible to achieve the same compaction pressure of the previous samples because the maximum load allowed by the hydraulic press was 10 tons and the cross-sectional area of the block is larger than the cylindrical specimens. This block was made using 60% of cement and 40% of water. After drying the block, four cylindrical samples were plugged.

Experimental Procedure

Petrophysical Measurements

Porosity of the artificial samples was measured using a Corelab Ultrapore-300 Helium porosimeter through grain volume measurements in a matrix cup at room conditions (API, 1998). Bulk volume was evaluated from caliper measurements. This method uses the Boyles law for estimating grain volume and allowing the evaluation of porosity.

Permeability of N₂ axial flow was measured using a Corelab PERG-200 steady-state permeameter at a confining pressure of 1000 PSI. No backpressure was applied, thus those measurements refer only to gas permeability (no Klinkenberg correction) according to Darcy's equation (Eq. 1).

$$1, \quad (1)$$

where k is the gas permeability, L is the length of the sample, A is cross-sectional area of the sample, μ is the gas viscosity, Q is the flow rate, \bar{p} is the mean pressure, p_1 is the inlet pressure and p_2 the outlet pressure (API, 1998).

Acoustic Measurements

P- and S-wave velocities were measured under uniaxial pressure of 3.5 MPa (~508 PSI) using ultrasonic transducers operating at 1.3 MHz (P-wave) and 900 KHz (S-wave) from the Rock Physics and Triaxial Deformation System at UENF. The pulse-transmission technique was used to estimate the velocities (Lima Neto et al., 2014) in the dry rocks. Lead foil was used for providing acoustic coupling.

Optical Microscopy and Digital Image Analysis

Optical microscopy (OM) in blue-epoxy resin impregnated thin-sections was performed using a Nova 148P transmitted light microscope. A Zeiss AxioCam HRC 13 MP digital camera was used for digital image acquisition. This equipment allowed a range from 40x up to 680x magnification.

Digital Image Analysis was made using ImageJ/Fiji software and consisted of contrast enhancement, segmentation and porosity evaluation. A Neural Network Algorithm called WEKA (ImageJ-Weka, 2016) was used for segmentation. That algorithm requires an assisted training prior to the segmentation, to accurately discriminate grains and pores. Such procedure results in a binary image, where the pores are represented as black pixels and matrix as white. The software can also evaluate the area covered by those black pixels. The ratio between such pore area and the total area of the image is assumed as the image porosity.

Results

Mineralogy

The materials (Portland cement, calcite powder and sand with grain sizes of 0.15 and 0.3mm) used for manufacturing the rock samples were analyzed using X-

ray Diffraction technique (XRD) for evaluating the mineral composition.

Table 2 presents values obtained by the XRD analysis. The percentage of mineral phases in each material was coherent with a specific mineral group of silicates (sand) and carbonates (calcite and cement). The sands have a major predominance of quartz (93% for the 0.15 mm grain size and 97.5% for the 0.3 mm grain size) representing the group of silicates and minor amounts of feldspar and mica. The calcite powder showed a predominance of calcite mineral (~ 90%) representing the carbonate phase and a small content of quartz. The Portland cement showed balanced percentages of the phases, with 40% of carbonate minerals associated with calcite and dolomite and a mixture of carbonates and silicates (60%) associated with Alite and Hatrurite minerals, which are calcium silicates (tricalcium aluminate and calcium aluminoferrite). These minerals are frequently generated in situ by the heating of various types of clays and limestones that originate the clinker during the fabrication process of Portland cement.

Porosity, permeability and velocities

Figure 1 shows a comparison of the three methods in terms of the variation of porosity and permeability versus the quantity of cementing fluid. The results showed that porosity decreases in a linear trend by the increasing amount of cementing fluid while permeability decreases in an exponential trend by this increasing.

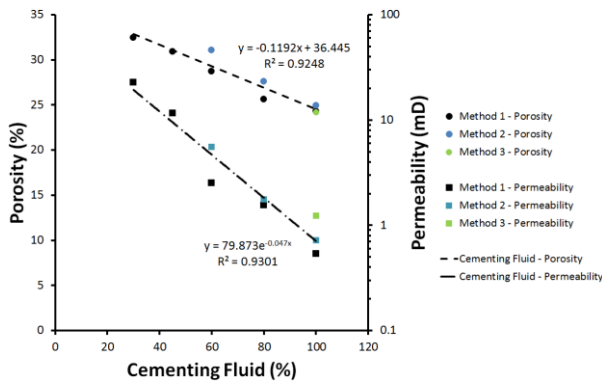


Figure 1: Porosity and permeability versus cementing fluid (all the methods).

Figure 2 shows the behavior of the P- and S-wave velocities with the increasing of cementing material. As expected, the velocities tend to increase when the porosity decreases with the addition of cementing fluid. The trend line shows that the variation is practically linear since the correlation coefficient is still high, but lower than those observed in correlations to porosity and permeability. The behavior of the ratio Vp/Vs for the studied samples is illustrated in Figure 3. The expectation was that its value would stay around 1.7 (Mavko et al. (2009)). As noted, the artificial samples showed ratio values Vp/Vs very close to natural samples.

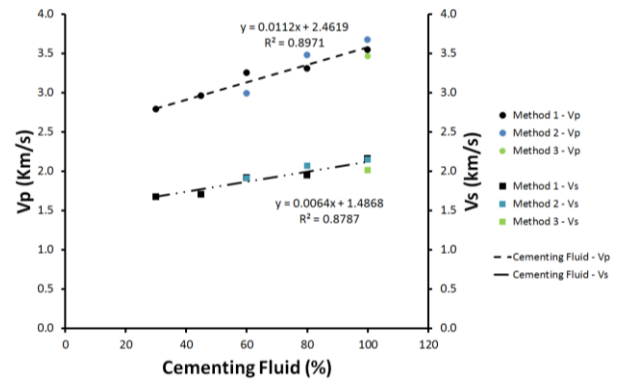


Figure 2: Vp and Vs versus cementing fluid (all the methods).

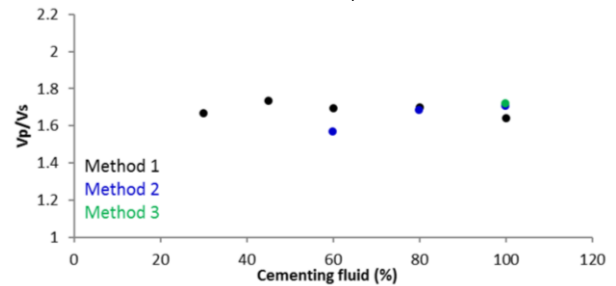


Figure 3: Vp/Vs versus cementing fluid (all the methods).

Optical Microscopy

The optical microscopy (OM) analysis was performed on the five samples made by the first method. According to Anselmetti et al. (1998), macropores are defined as those having diameter ≥ 20 μm, while smaller pores are assumed as micropores.

The samples were analyzed at 400x magnification. In each sample, four micrographs were taken in different positions of the thin-section. The image porosity of each sample was calculated by the arithmetic average of the values obtained in the four binary images. Figure 4 shows one representative micrograph of each sample.

The porosity obtained from the image analysis was compared with the porosity values evaluated by the Helium gas porosimetry. These results (Figure 4) reported that the porosity obtained through OM is smaller than those obtained through Helium gas porosimetry. At 400x magnification, the digital images have a resolution of 0.23 μm/pixel. A pore is defined by at least two pixels. Therefore, due to that resolution limitation, smaller pores cannot be observed by this method. The discrepancy between those two curves may also indicate the fraction of microporosity that is not inferred by OM. As a general trend, the lower the cementing fluid amount, the smaller the microporosity content. Such behavior is probably due to gaps in the cementation of the interparticle pore space. The increasing of the cement fluid content enhances the cementation, reduces the gap size and creates micropores.

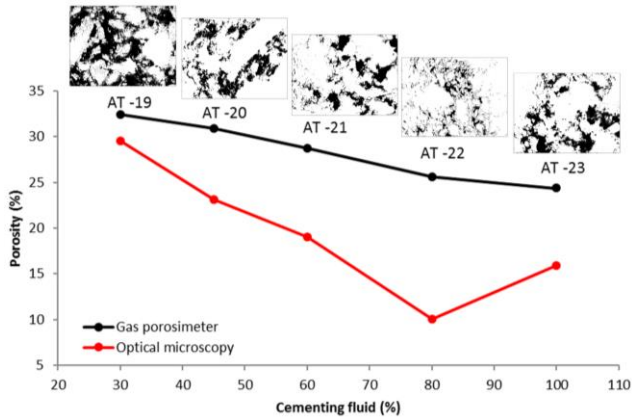


Figure 4: Porosities of the samples AT-19, AT-20, AT-21, AT-22 and AT-23. The black line corresponds to the porosity obtained from the Helium gas porosimeter. The red line corresponds to the porosity obtained by optical microscopy.

Comparison between synthetic and natural carbonate rocks

The permo-porosity behavior of the synthetic samples was plotted according to the methodology proposed by Lucia (1995) for characterizing natural carbonate rocks as can be seen in Figure 5. Data of Class 3 natural carbonates (Lucia, 1995) and the synthetic rocks are displayed in the same graphic. That result also indicates a similar behavior to the mud-dominated fabric carbonates.

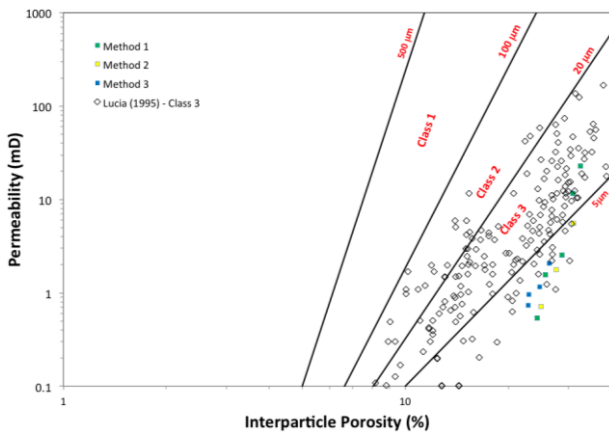


Figure 5: Crossplot of Interparticle Porosity and Gas Permeability according Lucia (1995) classification. Diamonds are related to measurements on Class 3 – Mud-dominated fabrics natural rocks (Lucia, 1995) and colored squares are related to the synthetic rocks.

Figure 6 shows the relationship between permeability and porosity of the synthetic samples and natural rocks mentioned by Archilha et al. (2013) and Røgen et al. (2005) comprising grainstones, cemented grainstones and mudstones. The synthetic samples with

porosity range between 20% and 30% are similar to mudstones.

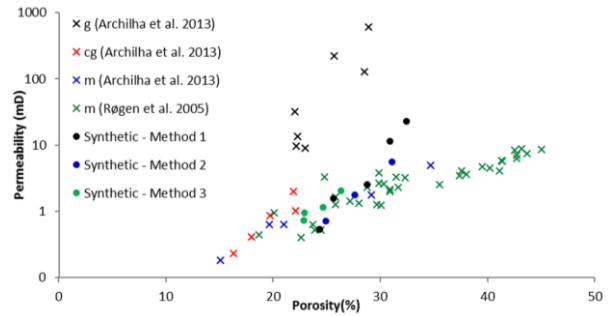


Figure 6: Comparison between permeability and porosity of natural and artificial samples; g: grainstones, cg: cemented grainstones, m: mudstones.

In Figure 7, V_p and V_s of synthetic rocks are compared with mudstone data (Røgen et al., 2005; Lima Neto et al, 2015), showing that these values are very similar and display practically the same linear trend. Main divergences may be due to differences in the confining pressure, because both works used a hydrostatic pressure of 7.5 MPa while measurements of the synthetic samples were performed at a 3.5 MPa uniaxial pressure.

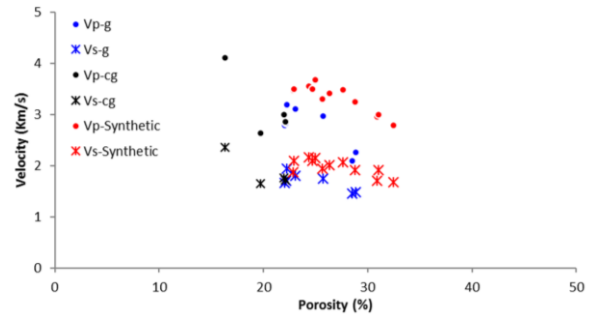


Figure 7: Comparison between velocity and porosity of natural (Lima Neto et al., 2014) and artificial samples; g: grainstones, cg: cemented grainstones.

Conclusions

The relationship between the cementing fluid content, porosity and permeability in the synthetic rocks could be evaluated through the analysis of the crossplots and the resulting regressions returned a high R^2 . The increasing of the cementing fluid content works to stiff the samples and to decrease both porosity and permeability.

As showed by mercury porosimetry and optical microscopy, the artificial samples have a primary microporosity. That feature provides a major impact in permeability, because the straight pore-throats tend to hamper the fluid flow through the rock. However, natural carbonate rocks may also include secondary porosity as vugs and fractures, which could alter significantly the permeability values.

The block plugs, which were constructed at a lower compaction pressure, showed a similar value of porosity, but a higher value of permeability. For all the

samples, porosity decreased in a linear way while permeability decreased exponentially when the cementing fluid was increased. As expected, P- and S-wave velocities have increased with the reduction of porosity.

When compared with natural rocks, the artificial rocks showed similar petrophysical characteristics of the mudstones, especially for the porosity range between 20-30%. In this case, such poro-permeability and poro-elastic velocities trends exhibited the same behavior of the mudstones as reported in the literature. Despite the differences between natural rocks cement and artificial Portland cement, the results indicate the feasibility of such synthetic rocks to be used as mudstone analogs. This methodology enables the construction of synthetic mudstone rocks through a fast and low-cost manner, which are adequate for petrophysical and rock physics experiments.

From a geological point of view, those results highlight the influence of the cementation as a key-controlling factor of the permo-porosity behavior of the mud-dominated fabric carbonate rocks.

Acknowledgments

We thank UENF/LENEP, PRH-ANP-20, CAPES, and PRH-PETROBRAS-226 to sponsor this study; Lorena Figueiredo, Luiz Abreu and Remilson Rosa for their help during the experiments; Abel Carrasquilla, Wagner Lupinacci, Nathaly Archilha and Marcelo Raso for valuable discussions.

References

- ANSELMETTI, F. S., LUTHI, S. M., EBERLI, G. P. 1998. Quantitative characterization of carbonate pore systems by digital image analysis. **AAPG Bulletin**, v. 82, n. 10, p. 1815-1836.
- API, 1998. Recommend Practices for Core Analysis. RP-40. **American Petroleum Institute**. 2nd Edition.
- ARCHILHA, N., MISSÁGIA, R., DE CEIA, M., LIMA NETO, I., DE CASTRO, L., DE SOUZA, F. 2013. Petrophysical, mineralogical, and P-wave velocity characterization of Albian carbonates from Campos Basin, Brazil. **SEG Technical Program Expanded Abstracts**, p. 2989-2993. doi: 10.1190/segam2013-0676.1
- DAVID, C., MENÉNDEZ, B., BERNABÉ, Y. The mechanical behaviour of synthetic sandstone with varying brittle cement content. **International Journal of Rock Mechanics and Mining Sciences**, v. 35, n. 6, p. 759–770, 1998. doi: 10.1016/S0148-9062(98)00003-5
- DEN BROK, S. W. J., DAVID, C., BERNABÉ, Y. 1997. Preparation of synthetic sandstones with variable cementation for studying the physical properties of granular rocks. **Comptes Rendus de l'Académie des Sciences - Series IIA - Earth and Planetary Science**, v. 325, n. 7, p. 487–492.
- EL HUSSEINY, A., VANORIO, T. 2015. The effect of micrite content on the acoustic velocity of carbonate rocks. **Geophysics**, 80, 4, JUL-AUG, p. L45-L55. doi: 10.1190/GEO2014-0599.1
- IMAGEJ-WEKA. 2016. Website: http://imagej.net/Trainable_Weka_Segmentation. Accessed in APR 01.
- LIMA NETO, I., MISSÁGIA, R., DE CEIA, M., ARCHILHA, N., OLIVEIRA, L. 2013. Dual pore system evaluation of Albian grainstone carbonates from Brazil using effective elastic media theory models. **SEG Technical Program Expanded Abstracts**, p. 2994-2998. doi: 10.1190/segam2013-0652.1
- LIMA NETO, I., MISSÁGIA, R., DE CEIA, M., ARCHILHA, N., OLIVEIRA, L. 2014. Carbonate pore system evaluation using the velocity–porosity–pressure relationship, digital image analysis, and differential effective medium theory. **Journal of Applied Geophysics**, v. 110, p. 23–33. doi:10.1016/j.jappgeo.2014.08.013
- LIMA NETO, I., MISSÁGIA, R., DE CEIA, M., ARCHILHA, N., HOLLIS, C. 2015. Evaluation of carbonate pore system under texture control for prediction of microporosity aspect ratio and shear wave velocity. **Sedimentary Geology**, v. 323, p. 43–65. doi: 10.1016/j.sedgeo.2015.04.011
- LUCIA, F.J. 1995. Rock-Fabric/Petrophysical Classification of Carbonate Pore Space for Reservoir Characterization. **AAPG Bull.** V. 79, No. 9 (September), P. 1275–1300.
- NIRLAULA, L. D. 2004. Development of modified t-z curves for large diameter piles/drilled shafts in limestone for Fb-pier. **M.Sc. thesis, University of Florida**, Florida, p. 163.
- PIANE, C. D., CLENNEL, M. B., DAUTRIAT, J., PRICE, G. 2015. Fluid/Rock Interactions in Porous carbonate Rocks: An integrated Mechanical, Ultrasonic and Microstructural Study. **AAPG Datapages/Search and Discovery Article #41745**.
- RØGEN, B., FABRICIUS, I. L., JAPSEN, P., HØIER, C., MAVKO, G., PEDERSEN, J. M. 2005. Ultrasonic velocities of North Sea chalk samples — influence of porosity, fluid content and texture. **Geophysical Prospecting**, v. 53, p. 481–496. doi: 10.1111/j.1365-2478.2005.00485.x
- SACRAMENTO, R. N., YANG, Y., YOU, Z., WALDMANN, A., MARTINS, A.L., VAZ, A. S. L., ZITHA, P. L. J., BREDIKOVETSKY, P., 2015. Deep bed and cake filtration of two-size particle suspension in porous media. **Journal of Petroleum Science and Engineering**. 126, 201-210. <http://dx.doi.org/10.1016/j.petrol.2014.12.001>.
- TORSATER, O., LI, S., HENDRANINGRAT, L., 2013. A Coreflood Investigation of Nanofluid Enhanced Oil Recovery in Low-Medium Permeability Berea Sandstone. **SPE International Symposium on Oilfield Chemistry**, The Woodlands, TX. doi: 10.2118/164106-MS
- WANG, Z., WANG, R., WANG, F., QIU, H., Li, T. 2015.

Experiment study of pore structure effects on velocities in synthetic carbonate rocks. **Geophysics**. 80, 3, MAY-JUN, p. D207-D219. doi: 101190/GEO2014-0366.1

XU, S., PAYNE, M.A. 2009. Modeling elastic properties in carbonate rocks: **The Leading Edge**, 28(1), 66-74. doi:10.1190/1.3064148.

Table 1: Quantity and material percentages used in the three methods.

Method	Samples	Weight fraction (%)				Quantity (g)			
		Calcite	Sand	Cement	Water	Calcite	Sand	Cement	Water
1	AT-19	95	5	20	10	120	6	25.2	12.6
1	AT-20	95	5	30	15	120	6	37.8	18.9
1	AT-21	95	5	40	20	120	6	50.4	25.2
1	AT-22	95	5	50	30	120	6	63	37.8
1	AT-23	95	5	60	40	120	6	75.6	50.4
2	AT-25	95	5	60	40	120	6	75.6	50.4
2	AT-26	95	5	50	30	120	6	63.0	37.8
2	AT-27	95	5	40	20	120	6	50.4	25.2
3	Block	95	5	60	40	1200	60	756	504

Table 2: Percentage of mineral phases obtained by XRD analysis of the material used in the experimental samples.

Materials	Mineral Phase (%)						
	Silicates Phases			Carbonates Phases		Clinker compound Portland Cement	
	Quartz SiO ₂	Feldspar (microcline) KAlSi ₃ O ₈	Mica (biotite) K(Mg,Fe) ₃ (OH,F) ₂ (Al,Fe)Si ₃ O ₁₀	Calcite CaCO ₃	Dolomite CaMg(CO ₃) ₂	Alite (Ca ₃ SiO ₅)	Hatrurite (Ca ₃ SiO ₅)
Sand 0.15mm	93	1.4	5.6	0.0	0.0	0.0	0.0
Sand 0.30mm	97.5	1.4	1.0	0.0	0.0	0.0	0.0
Calcite	4.2	0.0	0.0	76.3	13.5	0.0	0.0
Cement	4.1	0.0	0.0	35.8	3.5	43.3	13.4